

Learning continuous-valued treatment effects through representation balancing

Christopher Bockel-Rickermann^{*} Toon Vanderschueren^{*} Jeroen Berrevoets[†]
Tim Verdonck^{‡§} Wouter Verbeke^{*}

September, 2023

Abstract

Estimating the effects of treatments with an associated dose on an instance’s outcome, the “dose response”, is relevant in a variety of domains, from healthcare to business, economics, and beyond. Such effects, also known as continuous-valued treatment effects, are typically estimated from observational data, which may be subject to dose selection bias. This means that the allocation of doses depends on pre-treatment covariates. Previous studies have shown that conventional machine learning approaches fail to learn accurate individual estimates of dose responses under the presence of dose selection bias. In this work, we propose CBRNet, a causal machine learning approach to estimate an individual dose response from observational data. CBRNet adopts the Neyman-Rubin potential outcome framework and extends the concept of balanced representation learning for overcoming selection bias to continuous-valued treatments. Our work is the first to apply representation balancing in a continuous-valued treatment setting. We evaluate our method on a newly proposed benchmark. Our experiments demonstrate CBRNet’s ability to accurately learn treatment effects under selection bias and competitive performance with respect to other state-of-the-art methods.

Keywords: Causal Machine Learning, Potential Outcomes, Neyman-Rubin, Balanced Representation Learning, Dose Response

1 Introduction

Across domains, understanding the effects of treatments with an associated dose on the outcome of an instance is of key interest for personalized decision-making [1, 2]. Applications span across, e.g., healthcare, public policy, economics, and manufacturing [3–6]. However, learning such an effect (also known as the “individual dose response”, or “continuous-valued treatment effect”) is difficult for two main reasons. First, only factual observations are available for modeling, that is, every observation is observed in combination with just one “factual” dose and no other “counterfactuals”. This is commonly known as the “fundamental problem of causal inference” [7]. Second, the training data is typically observational and therefore suffers from various types of bias [8].

^{*}Faculty of Economics and Business, KU Leuven

[†]Department of Applied Mathematics and Theoretical Physics, University of Cambridge

[‡]Department of Mathematics, University of Antwerp - imec

[§]Department of Mathematics, KU Leuven

In this work, we investigate the problem of learning individual dose responses in the presence of dose selection bias. Dose selection bias and, more generally, treatment selection bias occurs when treatment assignment follows some policy based on the characteristics of an observation [9]. In such an environment, finding an unbiased estimator of a treatment effect is a complicated task where conventional supervised learning methods may fail [10]. Therefore, previous work has proposed specialized methodologies to deal with the effect of observational data in settings with continuous-valued treatments [1, 3, 4, 6, 11–17]. Yet, many of these methods are suited only for specific use cases (e.g., policy evaluation), rely on strict parametric assumptions, or are increasingly complex in their architecture, potentially hindering real-world implementation.

When training conventional machine learning algorithms, dose selection bias could lead to overfitting training observations for a particular dose interval [3] and consequently low generalization performance for counterfactual inference. To tackle this problem, we propose CBRNet, a method for **C**ontinuously-valued treatment effect estimation through **B**alanced **R**epresentation learning with neural **N**etworks. We build on recent advancements in representation learning and argue that, in order to find a well-functioning and unbiased model of individual dose response, we can find a balanced representation of the training data that is independent of the assigned dose. We hypothesize that this approach is also an effective solution to losing the influence of the dose on the outcome in high-dimensional latent space when training neural networks with multiple hidden layers [3, 10]. CBRNet clusters observations based on their pre-treatment covariates, and balances the data based on distances between clusters in latent space, hereby generalizing the approach presented in [10] the continuous-valued treatment setting.

To evaluate the capabilities of CBRNet, we develop a novel benchmark for simulating different levels of dose selection bias. We extend the experiments of Bica et al. [4], by shedding light on the drivers of selection bias that have not been under control in previous benchmarks. We test our methods against established methods for dose response estimation and show that CBRNet is performing competitively against the state of the art. Our contributions to the literature are as follows:

- we introduce CBRNet, a novel method for dose response estimation;
- we extend representation balancing to the continuous-valued treatment setting, and show how it may help to overcome the effects of selection bias;
- we propose a new benchmark for dose response learning, enabling a more comprehensive investigation of different aspects of dose selection bias in observational data;
- we conduct a series of experiments to understand the sensitivity of our method and existing methods and study the impacts of its different components on counterfactual inference and performance.

The remainder of this paper is organized as follows: First, in Section 2, we provide an overview of related literature. Then, in Section 3, we introduce the problem formulation. Subsequently, we illustrate and explain the workings of CBRNet in Section 4. Section 5 presents the results of extensive experiments to evaluate the proposed method. The paper is concluded in Section 7, which also provides an outlook on future work.

2 Related Works

The majority of literature on estimating treatment effects has been concerned with binary-valued treatments, that is, measuring the effect of applying a treatment, over not applying it [18, 19]. Less attention has been paid to settings with continuous-valued treatments. In these settings, an observation can be assigned an infinite amount of different treatment options by varying the dose of the treatment. Although less studied, such settings are of great importance in a variety of fields. These include personalized medicine [1, 4], public policy [20, 21], business and economics [22], manufacturing [5], or education [23].

The continuous-valued treatment setting further complicates learning treatment effects. Experimental evaluation of these effects through, for example, randomized controlled trials (RCTs) [24–26] is often infeasible due to both ethical concerns [27, 28] and the large number of possible treatment configurations compared to a limited number of candidates available for random assignment. As a result, the effects of continuous-valued treatments must usually be estimated from observational data, which comes with its own set of challenges.

We find two main fields of study with respect to continuous-valued treatments. First, the field of policy learning aims at deriving the optimal dose of a treatment, not necessarily considering the effects of other suboptimal doses. Recent work on policy evaluation for continuous-valued treatments includes [12–17]. Second, and the focus of our research, is the estimation of individual treatment effects (ITE). We base our research on the Neyman-Rubin potential outcomes framework [24, 29–31], and aim to estimate the effect of any possible dose of a treatment for a specific instance. A detailed formulation of our problem statement will be provided in Section 3.

Previous works take different approaches to tackling the estimation of dose responses. [1, 11, 32] use generalized propensity scores (GPS) to aid in the estimation of continuous-valued treatment effects. The GPS is defined as the probability of being assigned a certain dose of a treatment conditional on an observation’s pre-treatment covariates and is an extension to the propensity score proposed by [33] for binary-valued treatments. While not an estimate of the treatment effect itself, the GPS can be added to models in order to overcome dose selection bias. However, GPS calculation typically requires parametric assumptions that might not hold in real-life applications [34].

In recent years, we have seen the use of machine learning for the estimation of dose responses. [4] apply generative adversarial networks (GANs) to overcome dose selection bias. Their architecture SCIGAN works in three steps. First, a GAN is trained to generate counterfactuals for a given observation. Second, per training observation, the GAN produces a finite number of counterfactuals to augment the training data and to overcome selection bias. Third, a conventional machine learning method is trained to learn the dose response from the augmented data. Their approach generalizes the work of [35] for the case of continuous-valued treatments. However, as noted in [36], the application of generative methods is complicated, as, for example, the learning process requires optimizing intractable criteria. Combined with the general problem of evaluating and validating methods for treatment effect estimation (see again the “fundamental problem of causal inference” [7] and Section 5.2), we value the applicability of generative methods for causal inference as complicated, as convergence and correctness of a model is hard to achieve and verify. Schwab et al. [37] extend the work of Shalit et al. [10] in proposing a neural network architecture with a finite number of individual heads for estimating discretely-valued treatments. This idea is taken advantage of by [3] to propose DRNet. DRNet, for a single continuous-valued

treatment, trains a finite number E of head networks, all sharing a number of hidden layers. Each head network is trained to predict the outcome of one of E equally sized intervals of the observed range of doses. The strength of DRNet lies in the potential to learn highly flexible (and potentially different) models for different dose intervals [4]. Finally, Nie et al. [6] propose VCNet as a response to DRNet and address both DRNet’s inflexible approach to dividing the dose space into equally-sized intervals and its tendency to produce discontinuous estimates of dose response. VCNet builds on a varying-coefficient model [38]. In this architecture, a first neural network with a number of shared layers is trained to estimate a generalized propensity score. Then, a second inference network is trained, which takes as input the generalized propensity score estimate and varies its network coefficients as a function of the assigned dose. Under correct specification, DRNet is expected to be a special case of VCNet.

None of the previously established approaches, to the best of our knowledge, leverages representation balancing as used in the counterfactual regression framework (CFR) in Shalit et al. [10]. Therefore, our method is the first to generalize the idea of representation balancing for counterfactual inference to the continuous-valued treatment setting. Additionally, we present an architecture that is significantly simpler than the previously established causal machine learning methods. Instead of added flexibility along different dose levels (as in DRNet and VCNet), using a GPS estimate (VCNet and HIE), or generative methods (SCIGAN), the proposed method addresses selection bias during training. Our method provides a trade-off between (eventually overly simplistic) parametric assumptions and architectural complexity.

3 Problem formulation

We consider a situation in which subjects may receive a treatment with a continuous-valued dose, and in which one is interested in learning the impact of such treatment on an outcome from observational data.

Suppose historical data is observed in the form of $(\mathbf{x}_i, s_{i,f}, y_{i,f})$ for $i = 1, \dots, N$. Each of N observations consists of pre-treatment covariates \mathbf{x}_i , the assigned dose of the treatment $s_{i,f}$, and the outcome of this treatment-dose combination $y_{i,f}$. We make the following assumptions: \mathbf{x}_i is a realization of random variable \mathbf{X} , defined as the vector of pre-treatment covariates in feature space \mathcal{X} . $s_{i,f}$ is the observed dose of the treatment associated with observation i , realized from random variable $S_f \in \mathcal{S}$. $y_{i,f}$ is the observed outcome of the treatment with observed dose $s_{i,f}$ associated with observation i , realized from random variable $Y_f \in \mathcal{Y}$. We assume dose selection bias, meaning that the pre-treatment covariates of an observation confound the distribution of the factual dose. We follow Richardson et al. [39] and express the causal dependencies in the data as a single world intervention graph (SWIG), visualized in Figure 1.

We will continue to refer to all observed data as “factual” observations (denoted by subscript f), and to all unobserved combinations of instances and doses as “counterfactuals”.

We follow the Neyman-Rubin potential outcome framework [24, 29–31], with a unique outcome $Y(s, \mathbf{x})$ for every combination of pre-treatment covariates \mathbf{x} and dose s in some domain of interest \mathcal{S} . We are interested in finding an unbiased estimate of the outcome of a treatment-dose pair conditional on an observation’s pre-covariates, that is, the individual dose response:

$$\mu(s, \mathbf{x}) = \mathbb{E}(Y(s) | \mathbf{X} = \mathbf{x}). \quad (1)$$

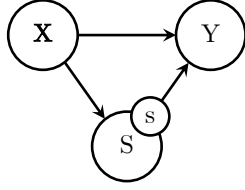


Figure 1: SWIG representing the causal dependencies between variables in the training data

We make three standard assumptions that are necessary for the identification of $\mu(d, \mathbf{x})$ from observational data [1, 40]:

Assumption 1. Unconfoundedness: *The assigned dose s and the potential outcome $Y(s)$ are conditionally independent given the pre-treatment covariates \mathbf{X} , or formally (cf. Figure 1):*

$$\{Y(s) | s \in \mathcal{S}\} \perp\!\!\!\perp S_f | \mathbf{X}$$

Assumption 2. Overlap: *Every observable combination of pre-treatment covariates \mathbf{x} has a non-zero probability of being assigned any of the possible doses s , or formally:*

$$\forall \mathbf{x} \in \mathcal{X} \text{ such that } \mathbb{P}(\mathbf{x}) > 0, \text{ we have } 0 < \mathbb{P}(s | \mathbf{x}) < 1 \text{ for each } s \in \mathcal{S}$$

Assumption 3. Consistency: *The factually observed outcome of a pair of pre-treatment covariates \mathbf{x} is unaffected by the assignment of doses to other observations, i.e., the observed factual outcome is the true potential outcome, or formally:*

$$\forall \mathbf{x} \in \mathcal{X} : Y_f = (Y | \mathbf{X} = \mathbf{x})$$

4 CBRNet

4.1 Motivation

Dose selection bias in observational data typically stems from the existence of an established (unknown) treatment assignment mechanism, resulting in confounding [18, 41, 42]. In business applications, for instance, these assignment mechanisms may be driven by corporate policy, such as a pricing policy [43]. Such a pricing policy might entail customer segmentation [44], under which specific customer segments are assigned different prices. This is often the case in, for example, the pricing of loan and insurance products [45]. Such customer segmentation finds clusters of customers that share certain characteristics. In effect, observations that are similar (as evaluated using some similarity metric), typically get assigned a similar dose of a treatment (e.g., a price for an insurance product, or credit rate for a loan). Consequently, observations from different clusters get assigned different doses, resulting in dose selection bias. Differences in pre-treatment covariates of the observations immediately drive the bias. We illustrate such a setting in Figure 2. Similar scenarios are found in various other applications, such as drug dose policies in healthcare or tax rate policies in economics.

The presence of such confounding complicates the learning of causal effects and requires careful algorithm design [46]. A machine learning algorithm could potentially overfit training

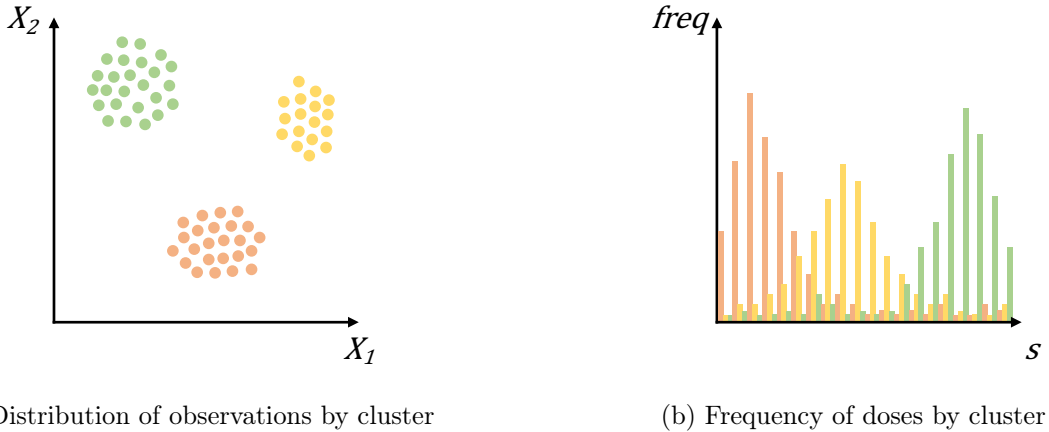


Figure 2: Illustrative visualization dose selection bias

observations that are not randomly sampled for specific dose levels. In particular, under the presence of strong dose selection bias, a machine learning method can learn to infer the dose (or the treatment option more generally) from an observation’s pre-treatment covariates. This will result in suboptimal generalization for counterfactual inference [3]. Further, the impact of the dose parameter on the outcome could get lost in high-dimensional latent space [3, 10].

In the binary-valued treatment setting, the seminal counterfactual regression framework (CFR) of [10] addresses this issue by first learning a balanced representation of the pre-treatment covariates of the training data which is invariant of the treatment option. Their approach regularizes in latent space the distance between observations that were treated and those that were untreated. Distance is measured using an integral probability metric (IPM) [47, 48]. After this regularization, the treatment option can no longer be inferred from an observation’s pre-treatment covariates, as such preventing overfitting.

The continuous-valued treatment setting complicates this approach, as observations cannot trivially be split into two (or multiple) groups by means of the treatment option. In fact, there is an infinite amount of possible groupings based on the assigned dose. Yet, as we expect similar instances to be assigned similar doses, we expect that clusters in the data are informative about the dose assignment, offering an alternative way of splitting training data for representation balancing.

Hence, we propose to find clusters in the data based on the pre-treatment covariates of an observation (as well as the assigned dose level). If the pre-treatment covariates of an observation are driving dose selection bias (i.e., if an established dose assignment policy was based on clusters, or could be approximated by such), finding clusters will enable us to find observations with similar doses. Reducing the distance between clusters in latent space should aid in dealing with bias for counterfactual inference. Such an approach will allow building models which are simple in their architecture, and which differ from conventional methods only in training. We propose CBRNet to be a standard feed-forward neural network, eliminating the need for multiple prediction head networks as in DRNet, or generative methods as in SCIGAN.

4.2 Architecture

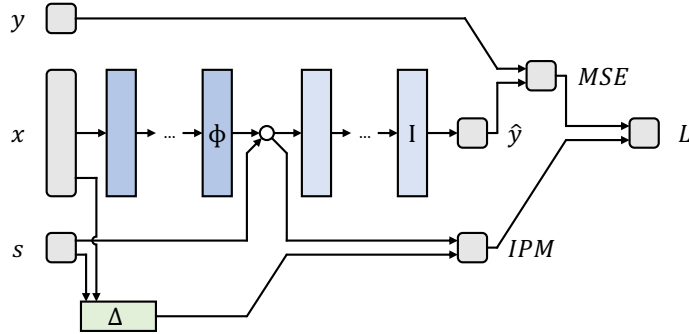


Figure 3: Architecture of CBRNet

We visualize the architecture of CBRNet in Figure 3. CBRNet consists of three parts Φ , Δ , and I , based on our motivation for such a method above. $\Phi : \mathcal{X} \rightarrow \mathbb{R}^n$ is a representation learning function that is in place to learn the balanced representation of the data. It is mapping the pre-treatment covariates into n -dimensional latent space. We use a standard feed-forward neural network for Φ , where both the number of layers and the number of hidden nodes per layer are hyperparameters. This is motivated by [10], yet other approaches are possible [49]. $\Delta : \mathcal{X} \times \mathcal{S} \rightarrow \{1, \dots, k\}$ is a clustering function mapping an observation to one of k clusters by taking as input the concatenated pre-treatment covariates and doses of an observation. Δ serves to identify clusters stemming from an assignment policy and could be any clustering function (for an overview see, e.g., [50]). We propose to use a k-means clustering [51], where k is a hyperparameter. K-means clustering has previously been used in treatment effect estimation in, e.g., [52]. The motivation to use k-means for CBRNet lies in minimizing Euclidian distances between observations of a certain cluster, as well as in wide adoption in business and beyond [53], expecting that k-means can approximate well the clusters generated from a potential ground-truth dose assignment mechanism. We train Δ on available training observations. Δ is not altered during the training of the remaining network components (see paragraph below). $I : \mathbb{R}^n \times \mathcal{S} \rightarrow \mathbb{R}$ is an inference function taking as input the transformed pre-treatment covariates (as given by Φ) and a dose. I is put in place to learn the final dose response model. As for Φ , we propose I to be a feed-forward neural network with flexible hyperparameters, as adopted in [3, 4, 10], and motivated by their flexibility for inference tasks [54]. However, in principle, any other inference method could be used (for an overview, see, e.g., [55]).

Training: CBRNet is trained by minimizing a loss L over a data set \mathcal{D} of training observations. L is defined as:

$$L(\mathbf{x}, s, y) = MSE(y, \hat{y}) + \lambda * R(\Phi, \Delta, \mathcal{D}) \quad (2)$$

$MSE(y, \hat{y})$ is a standard mean squared error loss over all N training observations:

$$MSE(y, \hat{y}) = \frac{1}{N} \sum_{i=1}^N (y_i - \hat{y}_i)^2 \quad (3)$$

y_i is the true outcome of observation i , \hat{y}_i is the estimated outcome and is calculated by the inference function I . The representation balancing of CBRNet is enforced by a regularization term R with a tuning parameter λ . We generalize previous work from [10] and calculate R as a combination of integral probability metrics over clusters identified by $\Delta(\cdot)$:

$$R(\Phi, \Delta, \mathcal{D}) = \frac{1}{k} \sum_{i=1}^k IPM \left(\{\Phi(\mathbf{x}_j, s_j)\}_{j:\Delta(\mathbf{x}_j, s_j)=i}, \{\Phi(\mathbf{x}_j, s_j)\}_{\mathbf{x}_j, s_j \in \mathcal{D}} \right) \quad (4)$$

k is the number of clusters found by $\Delta(\cdot)$, and IPM is any integral probability metric. In our proposal, $R(\cdot)$ compares the distribution of each cluster with the distribution of the total training data set \mathcal{D} , and regularizes accordingly. This approach is grounded in the assumption that the pre-treatment covariates in training data set \mathcal{D} are unbiased, and that regularizing cluster distributions to match the distribution of the total population will have an effective balancing effect. While any IPM could be used, e.g., a Wasserstein metric [56, 57], we propose using the mean maximum discrepancy (MMD) metric [58] due to the computational complexity of its empirical approximation. We combine the MMD with a radial basis function kernel for better balancing performance [59]. The regularizing effect of $R(\cdot)$ on Φ is visualized in Figure 4.

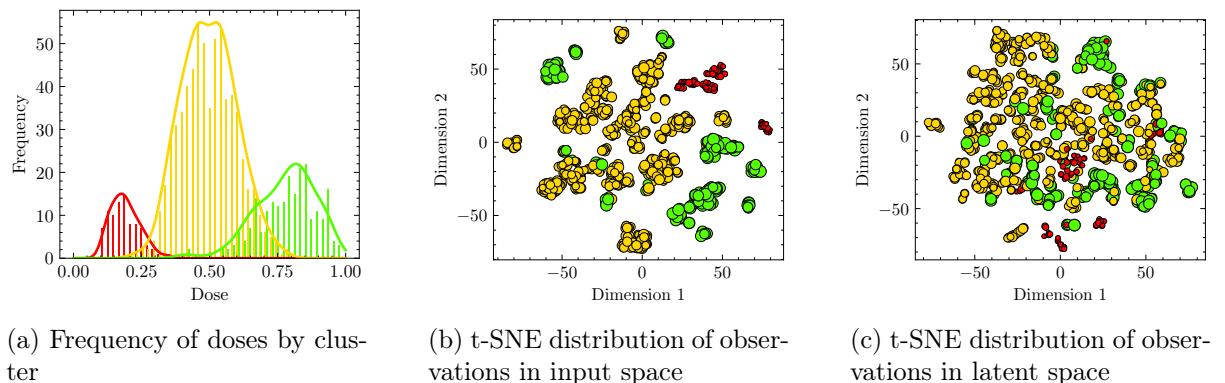


Figure 4: t-SNE visualization of pre-treatment covariates and their hidden representation

Hyperparameter tuning: Conventional machine learning research has established best practices for hyperparameter tuning and model selection, such as cross-validation [60]. However, these techniques cannot be applied immediately for the estimation of treatment effects, as predicting factual outcomes does not ensure performance on counterfactuals. As counterfactuals are unobserved and validation data are typically subject to the same levels of dose selection bias as training data, alternative methods for hyperparameter tuning and model selection must be used.

The previously discussed SCIGAN architecture [4] (cf. Section 2) circumvents this issue by generating counterfactuals to a validation set via a GAN. Alternatively, [3] propose a nearest-neighbor type method to calculate errors in estimating counterfactual outcomes. Their approach, however, may suffer from data sparsity for high dimensional problems, and likewise from increasing levels of selection bias.

Instead, we follow and extend [61]. For the binary-valued treatment setting, they propose to evaluate models based on a weighted mean squared error on a validation set, where observations

are weighted using an inverse of a propensity score estimate. This approach was chosen to give a higher weight to observations with a lower propensity, mimicking a counterfactual evaluation.

We extend to the continuous-valued treatment setting and propose to evaluate model performance via:

$$MSE_{val}(y, \hat{y}, \pi) = \sum_{i=1}^N \pi_i \sum_{i=1}^N \frac{1}{\pi_i} (y_i - \hat{y}_i)^2 \quad (5)$$

π_i is the generalized propensity score (GPS) of observation i , used to reweight the importance of validation observations. CBRNet can be used with any GPS estimate. In our study, we choose the approach presented in [11] and calculate the generalized propensity score by modeling s as a linear function of the pre-treatment covariates, assuming normally-distributed errors.

5 Experimental Evaluation

In this section, we present an experimental evaluation of CBRNet. In Section 5.1, we present the experimental framework, including a novel process to generate semi-synthetic test data. Section 5.2 discusses evaluation metrics and the methods that are used for benchmarking. Section 5.3 will briefly discuss the implementation of methods and link to the source code. Our experimental results are presented in Section 6. Additionally, we evaluate the performance of CBRNets on previously established data sets in Section 6.1, and analyze hyperparameter robustness in Section 6.2.

5.1 Data generation

In order to enable thorough testing and evaluation of our method, we make use of semi-synthetic data. Using a real and nonaugmented data set would prevent testing the performance of CBRNets for counterfactual inference [3, 4] due to the fundamental problem of causal inference, that is, the unobservability of counterfactuals. Previously, [4] proposed an approach to generating test data for the estimation of continuous-valued treatment effects that we will take advantage of. The approach starts from a set of pre-treatment covariates. Further, every observation gets assigned a mode of possibly assigned doses as a linear combination of its pre-treatment covariates. The strength of the selection bias is subsequently controlled by sampling the assigned dose from a Beta-distribution with the observation’s mode, where variance is controlled via parameter α , the strength of the bias. If no bias is simulated, the Beta-distribution is equivalent to a uniform distribution over possible dose levels. Under maximum bias, every observation is assigned exactly the dose mode. For a full discussion see [4].

While arguably elegant, this data-generating process might not be representative of all real-world applications of treatment effect estimation, as the dose assignment is instance-dependent. Therefore, the distribution of observed doses is dependent on the distribution of the pre-treatment covariates in the input space \mathcal{X} . We expect this to have a critical impact on the complexity (or “hardness”) of the data for treatment effect estimation. We show in Figure 5 that for an elevated level of bias ($\alpha = 5$), the dose distribution for the data generated in [4] is unimodal, which might not be realistic for a multitude of settings in reality (e.g., pricing, as discussed previously).

We present an extension of this data-generating process that allows for cluster-centric dose assignment and multimodal dose distributions in the training data, in order to imitate many

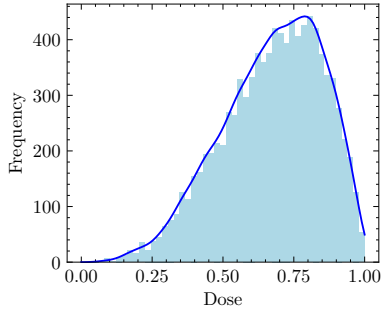


Figure 5: Distribution of doses in data of [4] with bias strength $\alpha = 5$

relevant real-world settings, and better control interlinked factors driving the effects of dose selection bias on treatment effect estimation. We also make use of the TCGA data set [62] due to its availability, high dimensionality, and wide adoption across research fields.

Step 1 (Clustering): The incoming pre-treatment covariates used for the data generation are clustered into a distinct number of clusters using k-means clustering. Specifically, we choose $k = 3$. For an observation i , we denote the corresponding cluster as c_i . This clustering mimics, for example, customer segmentation in a business context (see also the “News” data set first introduced in [63]), or patient segmentation in a medical context that might be used for a dose assignment.

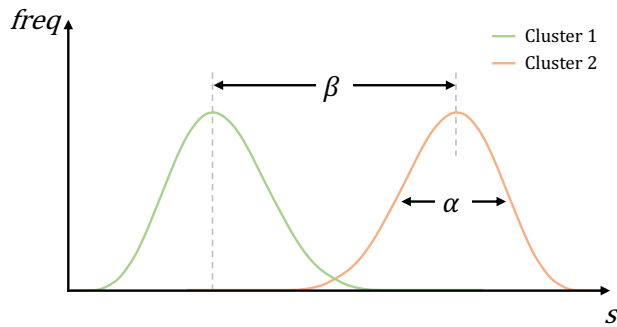
Step 2 (Dose assignment): We assign doses to clusters, instead of individual observations. This is a key difference to previous approaches, and yet again inspired by real-life data-generating processes. We consider two interlinked phenomena in observational data:

First, we will assign a certain modal dose to each cluster. Instead of modeling the modal dose as a combination of the pre-treatment covariates of each observation, we assign doses to clusters and control for the difference in modes between clusters. In previous approaches, this property of the data-generating process could not be controlled and is a quality of the chosen pre-treatment covariates. We will refer to this difference in doses between clusters as the “*inter-cluster dose variability*” (or for the case of [4] as the “*inter-observational dose variability*”). Specifically, we randomly assign each of the k clusters in our data to one of the k modal doses. Modal doses are evenly distributed along $[(1 - \beta)/2, (1 + \beta)/2]$. β is the parameter varying the inter-cluster variability, with $\beta = 0$ resulting in no variability and all clusters being assigned the same modal dose, and $\beta = 1$ resulting in maximal variability. The mode of cluster i is also referred to as m_i . Our approach allows to actively control the level of inter-cluster dose variability, while in [4] the variability is solely driven by the pre-treatment covariates.

Second, when assigned a certain dose, an observation can yet be assigned different levels of the latter due to randomness, or errors. This randomness is controlled in [4] with the parameter α , ranging from a completely random assignment of a dose unrelated to an assigned modal dose, to a fully deterministic assignment with every observation assigned the mode. Such variability is of crucial importance for the satisfaction of the overlap assumption discussed in Section 3. We will refer to this level of randomness as the “*intra-cluster dose variability*” (or for the case in [4] as the “*intra-observational dose variability*”). The intra-cluster dose variability is driven by the variable α , keeping the previously established notation. We enforce intra-cluster variability by

sampling the dose for each observation within a cluster from a Beta-distribution $\text{Beta}(1 + \alpha, \omega_i)$, with $\alpha \geq 0$, and $\omega_i = ((\alpha - 1)/m_{c_i}) + 2 - \alpha$. $\alpha = 0$ results in a uniform distribution, random assignment of the dose, and maximal intra-cluster variability. For $\alpha > 0$ the mode of the distribution is m_{c_i} . For $\alpha \rightarrow \infty$ the dose assignment becomes fully deterministic, so every observation within a cluster is assigned the cluster mode¹, and the intra-cluster variability is minimal.

To the best of our knowledge, our approach is first in differentiating the factors influencing dose selection bias in a systematic way, and could be combined with other data sets for domain-specific assessments of methods. For a visualization of the different components to the dose selection bias in our data, we add Figure 6. Figure A1 in the Appendix visualizes the dose distributions for some selected values of α and β .



Parameter β drives inter-cluster variability, i.e., the difference in modal doses between clusters. Parameter α drives the intra-cluster variability, i.e., the variance in assigning the modal dose.

Figure 6: Components of dose selection bias

Step 3 (Dose response calculation): After the final dose is sampled, the effect of treatment or the dose response is calculated using a ground truth model. While any functional form of the dose response is possible, we follow [4] and define for our experiments:

$$\mu(s, \mathbf{x}) = 10 ((\mathbf{w}_1)^\top \mathbf{x} + 12(\mathbf{w}_2)^\top \mathbf{x}s - 12(\mathbf{w}_3)^\top \mathbf{x}s^2) + \epsilon, \quad (6)$$

$\mathbf{w}_i \sim \mathcal{U}((0, 1)^{s \times 1})$ for $i \in \{1, 2, 3\}$ is a weight vector, $\epsilon \sim \mathcal{N}(0, 1)$ is an error term.

5.2 Benchmarking

We compare CBRNet against four benchmarking methods: 1) A standard multilayer perceptron (MLP), i.e., a feed-forward neural network that takes both pre-treatment covariates and the dose level as input of the first layers. MLPs are flexible and potent machine learning methods, that have seen wide application across domains, motivating their selection as a benchmark; 2) The Hirano Imbens estimator (HIE) [11], as parametric causal method; 3) DRNet and 4) VCNet, representing the state-of-the-art in continuous-valued treatment effect modeling.

For our experiments, we generate 10 iterations of the data set for each combination of different levels of $\alpha \in \{0, 3, 6, 9\}$ and $\beta \in \{0, 0.2, 0.4, 0.6, 0.8\}$. We then split the data set into a training

¹For a proof, see [4].

set (70%), a validation set (10%), and a test set (20%). We tune CBRNet and all benchmarking methods on each of the resulting 200 data sets and evaluate them via the mean integrated squared error (MISE) over all test observations and over all dose levels as proposed by [3]:

$$\text{MISE} = \frac{1}{N} \sum_{i=1}^N \int_{\mathcal{S}_f} (\mu(u, \mathbf{x}_i) - \hat{\mu}(u, \mathbf{x}_i))^2 du \quad (7)$$

5.3 Implementation

All experiments are implemented in Python 3.9. All neural network-based methods (MLP, DRNet, VCNet, and CBRNet) are implemented in *PyTorch* [64]. MLP and CBRNet use our own implementation, VCNet is built on the original code provided by [6]. The HIE model is implemented using the *statsmodels* library [65] and is inspired by the implementation of the method in the *causaldrf* package [66] for the statistical programming language *R* [67]. Hyperparameters for all methods but CBRNet are tuned based on their mean squared error (MSE) on a validation set. A list of hyperparameters considered per model can be found in Section A. All code used for this project is available online via:

<https://github.com/christopher-br/CRBNet>

6 Experimental results

Table 1: MISE per method for $\alpha = 3.0$ and varying levels of β

$\alpha = 3.0$					
Model	β				
	0.0	0.2	0.4	0.6	0.8
MLP	1.42 ± 0.31	1.25 ± 0.30	1.19 ± 0.23	0.91 ± 0.18	0.97 ± 0.26
HIE	2.06 ± 0.04	2.05 ± 0.03	2.12 ± 0.10	2.34 ± 0.13	2.43 ± 0.11
DRNet	1.32 ± 0.10	1.15 ± 0.12	1.19 ± 0.21	0.95 ± 0.14	0.75 ± 0.09
VCNet	1.24 ± 0.07	1.12 ± 0.17	0.90 ± 0.21	0.64 ± 0.23	0.37 ± 0.16
CBRNet	0.97 ± 0.20	0.77 ± 0.15	0.57 ± 0.25	0.53 ± 0.13	0.39 ± 0.14

Table 2: MISE per method for $\beta = 0.4$ and varying levels of α

$\beta = 0.4$				
Model	α			
	0.0	3.0	6.0	9.0
MLP	0.54 ± 0.06	1.19 ± 0.23	1.65 ± 0.49	2.12 ± 0.39
HIE	0.71 ± 0.04	2.12 ± 0.10	2.65 ± 0.31	2.97 ± 0.36
DRNet	0.64 ± 0.02	1.19 ± 0.21	1.37 ± 0.11	1.62 ± 0.16
VCNet	0.19 ± 0.02	0.90 ± 0.21	1.38 ± 0.28	1.68 ± 0.27
CBRNet	0.29 ± 0.04	0.57 ± 0.25	0.96 ± 0.21	1.37 ± 0.18

In line with the data-generating process in Section 5, we present the performance of CBRNet along both a fixed level of intra-cluster dose variability ($\alpha = 3.0$, Table 1) and along a fixed level

of inter-cluster dose variability ($\beta = 0.4$, Table 2) averaged over 10 randomly initialized data sets per combination of α and β . Values in bold mark the best-performing model for a certain bias combination, and values in italics mark the second best. For performances under different levels of α and β , see Tables A4 and A5 in the appendix.

For a fixed level of intra-cluster dose variability, CBRNet outperforms benchmarks and is closely tied second only for the case of high inter-cluster variability. For the case of fixed inter-cluster dose variability, CBRNet is outperforming for all values of $\alpha > 0$. Only for the case of $\alpha = 0$, VCNet significantly outperforms CBRNet. This case mimics a randomized controlled trial. In aggregate, the results demonstrate that our approach of representation balancing for continuous-valued effect estimation is indeed effective, and competitive with the state of the art.

Additionally, the results allow to better understand the effects of the data-generating process, the impacts of inter- and intra-cluster variability on model performance, and the drivers of selection bias:

- For a fixed level of *inter*-cluster variability (fixing β), reducing the intra-cluster variability (i.e., increasing α) will complicate learning a dose response. This is mimicking the data-generating process of [4], hence this observation is expected.
- For a fixed level of *intra*-cluster variability (fixing α), varying inter-cluster variability (i.e., β) has a more complex effect. With no inter-cluster variability ($\beta = 0$), but some intra-cluster variability ($\alpha > 0$), the doses of all clusters are centered around a common mode, and for doses increasingly different from this mode, observations become increasingly sparse. In these situations, DRNet excels, due to its potential to learn potentially very different functions for separate dose intervals [3, 4]. The distribution of doses, however, is not driven by dose selection bias (i.e., confounding). Increasing inter-cluster variability now has two effects: 1) It *decreases* sparseness of observations across all dose levels, aiding the estimation of treatment effects. 2) It *increases* the effects of dose selection bias (confounding), deteriorating model performance. Figure A1 in the appendix is illustrating this phenomenon. This behavior results in first increasing, and later decreasing model performance for increasing levels of β for a fixed level of α .

6.1 Results on previously established data sets

We train and test CBRNet on the previously established data-generating process from [4] to evaluate performance on a different, recently proposed data-generating process. In this process, observations are not assigned doses per cluster, but rather individually, by first generating a unique modal dose per observation i :

$$s_i(\mathbf{x}) = (\mathbf{w}_4)^\top \mathbf{x} \quad (8)$$

with $\mathbf{w}_4 \sim \mathcal{U}((0, 1)^{s \times 1})$ a weight vector. The assigned dose is subsequently sampled from a Beta-distribution with such mode, as discussed for the experiments in Section 5.1. For benchmarking, we set the inter-observational variation (the bias level) to $\alpha = 5$, corresponding to a high level of bias (compared to the experiments in [4]). For the ground truth dose response, we consider all three options proposed in the original manuscript:

$$\text{GT \#1: } \mu(s, \mathbf{x}) = 10 \left((\mathbf{w}_1)^\top \mathbf{x} + 12(\mathbf{w}_2)^\top \mathbf{x}s - 12(\mathbf{w}_3)^\top \mathbf{x}s^2 \right) + \epsilon \quad (9)$$

$$\text{GT \#2: } \mu(s, \mathbf{x}) = 10 \left((\mathbf{w}_1)^\top \mathbf{x} + \sin\left(\pi \left(\frac{(\mathbf{w}_2)^\top \mathbf{x}}{(\mathbf{w}_3)^\top \mathbf{x}}\right) s\right) \right) + \epsilon \quad (10)$$

$$\text{GT \#3: } \mu(s, \mathbf{x}) = 10 \left((\mathbf{w}_1)^\top \mathbf{x} + 12s \left(s - 0.75 \frac{(\mathbf{w}_2)^\top \mathbf{x}}{(\mathbf{w}_3)^\top \mathbf{x}} \right)^2 \right) + \epsilon \quad (11)$$

Note that the original data-generating process generates observations to each of these ground truth models simultaneously. CBRNet is not designed to handle multiple distinct treatment options (though such an extension is feasible). We hence test the performance on each of the ground truth models individually².

As before, we generate 10 versions of the data sets, train benchmarking models, and average the MISE over all runs. The results in Table 3 show the competitive performance of CBRNet on all ground truth models, performing second best in two out of three cases, and consistently beating the standard MLP.

Table 3: MISE on data-generating process of [4] with $\alpha = 5$

Model	GT #1	GT #2	GT #3
MLP	2.045	1.240	3.147
DRNet	1.632	1.226	<i>2.975</i>
VCNet	2.120	0.717	2.135
CBRNet	<i>1.922</i>	<i>0.919</i>	3.012

6.2 Hyperparameter robustness and sensitivity

For training CBRNet, two key hyperparameters need to be set: The strength of the IPM regularisation λ , and the number of clusters to be identified by the k-means clustering k . We analyze the impact of varying these parameters on model performance in two experiments.

Impact of regularization strength λ : Figure 7 visualizes the impact of varying levels of regularization strength in the case without selection bias ($\alpha = 0$ and $\beta = 0$), and for elevated levels of selection bias ($\alpha = 5.0$ and $\beta = 0.5$). For each configuration, 10 data sets have been generated. Results are averaged over these iterations. We test two kinds of regularization. First, we test regularizing with a linear MMD. The linear MMD penalizes deviations of feature means across distributions but has little regularizing effects on a distribution’s shape or variance. Second, we test regularizing with a radial basis function kernel, as in our main experiments. The goal is to investigate the effects of different IPMs on the performance of CBRNet.

In the case without bias (cf. Figure 7a), model performance is seemingly unaffected by any level of λ . More so, increasing levels of λ indeed lower the MISE for both linear and kernel MMD regularization.

Suppose bias persists in the data (cf. Figure 7b). In that case we find the kernel MMD strictly improving model performance for $\lambda > 0$, whereas the linear MMD decreases model performance, especially for higher values of λ . For extreme values ($\lambda \in \{100, 500\}$) the linear MMD

²Note that we have not implemented the HIE, due to its low performance in the original manuscript, see for reference [4].

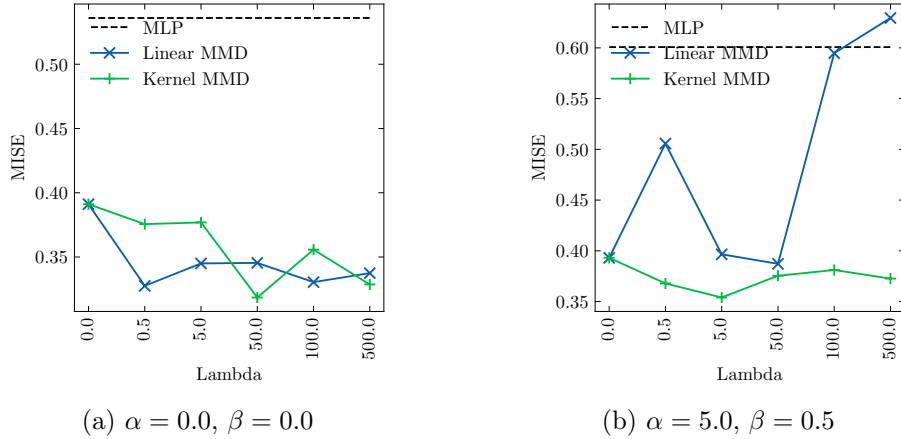


Figure 7: Impact of varying regularization strength λ on MISE

seemingly over-regularizes, resulting in model performance at par or below the conventional MLP benchmark.

These results support the need for model selection, as discussed in Section 4.

Impact of assumed number of clusters k : Figure 8 visualizes the effect of varying the number of assumed clusters for the k-means clustering in CBRNet. For this experiment, again an elevated level of bias was simulated ($\alpha = 5.0$ and $\beta = 0.5$) for 10 randomly generated data sets.

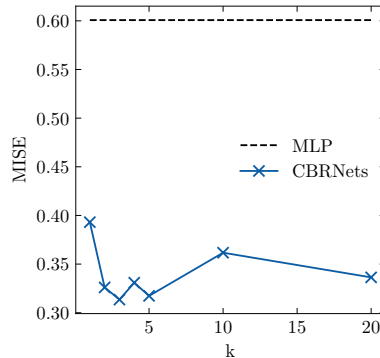


Figure 8: Impact of varying number of clusters k

We observe performance improvements of CBRNet over the conventional MLP benchmark across all selected numbers of clusters. Note that, for $k = 1$, we do not regularize the latent representation at all. Hence for any level of k balancing has a positive effect on the learned dose response. This is to be expected, as CBRNet regularizes each cluster distribution for deviations from the population, hence regularizing for more than the actual 3 clusters (as generated in the data) should have no significant adverse effect. As the MMD loss is calculated empirically, however, k should be chosen sufficiently small with respect to the batch size for network training to allow for adequate computation. We refer the interested reader to the source code (cf. Section 4). For applications of CBRNet, k can either be tuned or set based on expert assessment

7 Conclusion

We proposed CBRNet, a novel method for dose response learning from observational data. CBRNet builds on representation balancing and generalizes previously established architectures [10] to the continuous-valued treatment setting. CBRNet employs a simple feed-forward network architecture and achieves competitive performance by regularizing high-dimensional latent space with a custom loss over integral probability metrics.

Our approach enables representation balancing for continuous-valued treatments by clustering observations based on their pre-treatment covariates, instead of the assigned treatment option. Hereby, CBRNet is strongly inspired by real-world data-generating processes and in them, the reasons for dose selection bias and confounding.

In order to thoroughly evaluate CBRNet, we proposed a novel data-generating process that allows investigation of the interlinked factors that create dose selection bias. Hereby, we build and advance on the state of the art. Comparing CBRNet against both conventional machine learning benchmarks, as well as causal machine learning methods, we show increased robustness against dose selection bias and competitive performance of our model. We also conduct experiments on previously established benchmarking data sets, and evaluate the sensitivity of CBRNets to hyperparameter tuning, for which we provide selection criteria. All code is available online.

Compared to some of the existing dose response models (DRNet and SCIGAN), CBRNet is designed for data with only one treatment with a dose parameter in comparison to several, potentially very different treatment options, different versions of a treatment [68], or changes to treatment effects in time-dynamic environments [69]. Future research is to extend CBRNet to the multi-treatment setting, as well as on generating metrics that allow studying and understanding the presence and strength of selection bias in observational data.

Funding

This work was supported by the Research Foundation – Flanders (FWO research projects G015020N and 11I7322N).

JB is funded by the W.D. Armstrong Trust Fund.

Conflict of interest

The authors state no conflict of interest.

References

- [1] Imbens GW. The role of the propensity score in estimating dose-response functions. *Biometrika*. 2000;87(3):706-10.
- [2] Mueller S, Pearl J. Personalized decision making—A conceptual introduction. *J Causal Inference*. 2023;11(1):20220050.

- [3] Schwab P, Linhardt L, Bauer S, Buhmann JM, Karlen W. Learning counterfactual representations for estimating individual dose-response curves. In: Proceedings of the AAAI Conference on Artificial Intelligence. vol. 34; 2020. p. 5612-9.
- [4] Bica I, Jordon J, van der Schaar M. Estimating the effects of continuous-valued interventions using generative adversarial networks. *Adv Neural Inf Process Syst.* 2020;33:16434-45.
- [5] Vanderschueren T, Boute R, Verdonck T, Baesens B, Verbeke W. Optimizing the preventive maintenance frequency with causal machine learning. *Int J Prod Econ.* 2023;258:108798.
- [6] Nie L, Ye M, Liu Q, Nicolae D. Vcnet and functional targeted regularization for learning causal effects of continuous treatments. *arXiv preprint arXiv:210307861.* 2021.
- [7] Holland PW. Statistics and causal inference. *JASA.* 1986;81(396):945-60.
- [8] Hammerton G, Munafò MR. Causal inference with observational data: the need for triangulation of evidence. *Psychol Med.* 2021;51(4):563-78.
- [9] Tripepi G, Jager KJ, Dekker FW, Zoccali C. Selection bias and information bias in clinical research. *Nephron Clin Pract.* 2010;115(2):c94-9.
- [10] Shalit U, Johansson FD, Sontag D. Estimating individual treatment effect: generalization bounds and algorithms. In: *International Conference on Machine Learning.* PMLR; 2017. p. 3076-85.
- [11] Hirano K, Imbens GW. The propensity score with continuous treatments. *Applied Bayesian modeling and causal inference from incomplete-data perspectives.* 2004;226164:73-84.
- [12] Schweisthal J, Frauen D, Melnychuk V, Feuerriegel S. Reliable Off-Policy Learning for Dosage Combinations. *arXiv preprint arXiv:230519742.* 2023.
- [13] Krishnamurthy A, Langford J, Slivkins A, Zhang C. Contextual bandits with continuous actions: Smoothing, zooming, and adapting. *JMLR.* 2020;21(1):5402-46.
- [14] Kallus N, Zhou A. Policy evaluation and optimization with continuous treatments. In: *AISTATS.* PMLR; 2018. p. 1243-51.
- [15] Chen G, Zeng D, Kosorok MR. Personalized dose finding using outcome weighted learning. *JASA.* 2016;111(516):1509-21.
- [16] Zou H, Li B, Han J, Chen S, Ding X, Cui P. Counterfactual Prediction for Outcome-Oriented Treatments. In: *ICML.* PMLR; 2022. p. 27693-706.
- [17] Chernozhukov V, Demirer M, Lewis G, Syrgkanis V. Semi-parametric efficient policy learning with continuous actions. *NIPS.* 2019;32.
- [18] Imbens GW, Rubin DB. *Causal inference in statistics, social, and biomedical sciences.* Cambridge University Press; 2015.
- [19] Pearl J. *Causality.* Cambridge university press; 2009.

- [20] Kreif N, Grieve R, Díaz I, Harrison D. Evaluation of the effect of a continuous treatment: a machine learning approach with an application to treatment for traumatic brain injury. *Health Econ.* 2015;24(9):1213-28.
- [21] Michalek J, Ciaian P. Capitalization of the single payment scheme into land value: generalized propensity score evidence from the European Union. *Land Econ.* 2014;90(2):260-89.
- [22] Li Y, Palma MA, Hall CR, Khachatryan H, Capps Jr O. Measuring the effects of advertising on green industry sales: A generalized propensity score approach. *Appl Econ.* 2019;51(12):1303-18.
- [23] Kluve J, Schneider H, Uhlendorff A, Zhao Z. Evaluating continuous training programmes by using the generalized propensity score. *J R Stat Soc Ser A Stat Soc.* 2012;175(2):587-617.
- [24] Rubin DB. Estimating causal effects of treatments in randomized and nonrandomized studies. *J Educ Psychol.* 1974;66(5):688.
- [25] Angrist JD, Pischke JS. *Mostly harmless econometrics: An empiricist's companion.* Princeton university press; 2009.
- [26] Deaton A, Cartwright N. Understanding and misunderstanding randomized controlled trials. *Soc Sci Med.* 2018;210:2-21.
- [27] Schafer A. The ethics of the randomized clinical trial. *NEJM.* 1982;307(12):719-24.
- [28] Jamison JC. The entry of randomized assignment into the social sciences. *J Causal Inference.* 2019;7(1):20170025.
- [29] Neyman J. Sur les applications de la théorie des probabilités aux expériences agricoles: Essai des principes. *Roczniki Nauk Rolniczych.* 1923;10(1):1-51.
- [30] Rubin DB. Direct and indirect causal effects via potential outcomes. *Scand J Stat.* 2004;31(2):161-70.
- [31] Rubin DB. Causal inference using potential outcomes: Design, modeling, decisions. *JASA.* 2005;100(469):322-31.
- [32] Imai K, Van Dyk DA. Causal inference with general treatment regimes: Generalizing the propensity score. *JASA.* 2004;99(467):854-66.
- [33] Rosenbaum PR, Rubin DB. The central role of the propensity score in observational studies for causal effects. *Biometrika.* 1983;70(1):41-55.
- [34] Collier ZK, Leite WL, Karpyn A. Neural networks to estimate generalized propensity scores for continuous treatment doses. *Eval Rev.* 2021:0193841X21992199.
- [35] Yoon J, Jordon J, Van Der Schaar M. GANITE: Estimation of individualized treatment effects using generative adversarial nets. In: *International Conference on Learning Representations*; 2018. p. 1-22.
- [36] Goodfellow I, Bengio Y, Courville A. *Deep learning.* MIT press; 2016.

- [37] Schwab P, Linhardt L, Karlen W. Perfect match: A simple method for learning representations for counterfactual inference with neural networks. arXiv preprint arXiv:181000656. 2018.
- [38] Hastie T, Tibshirani R. Varying-coefficient models. *J R Stat Soc Series B Stat Methodol.* 1993;55(4):757-79.
- [39] Richardson TS, Robins JM. Single world intervention graphs (SWIGs): A unification of the counterfactual and graphical approaches to causality. Center for the Statistics and the Social Sciences, University of Washington Series Working Paper. 2013;128(30):2013.
- [40] Lechner M. Identification and estimation of causal effects of multiple treatments under the conditional independence assumption. Springer; 2001.
- [41] Rosenbaum PR, Rosenbaum P, Briskman. Design of observational studies. vol. 10. Springer; 2010.
- [42] Ellenberg JH. Selection bias in observational and experimental studies. *Stat Med.* 1994;13(5-7):557-67.
- [43] Phillips RL. Pricing and revenue optimization. Stanford university press; 2021.
- [44] Kung M, Monroe KB, Cox JL. Pricing on the Internet. *J Prod Brand Manag.* 2002;11(5):274-88.
- [45] Phillips R. Optimizing prices for consumer credit. *J Revenue Pricing Manag.* 2013;12:360-77.
- [46] Alaa A, van der Schaar M. Limits of estimating heterogeneous treatment effects: Guidelines for practical algorithm design. In: International Conference on Machine Learning. PMLR; 2018. p. 129-38.
- [47] Müller A. Integral probability metrics and their generating classes of functions. *Adv Appl-Probab.* 1997;29(2):429-43.
- [48] Sriperumbudur BK, Fukumizu K, Gretton A, Schölkopf B, Lanckriet GRG. On the empirical estimation of integral probability metrics. *EJS.* 2012;6:1550 1599.
- [49] Bengio Y, Courville A, Vincent P. Representation learning: A review and new perspectives. *IEEE Trans Pattern Anal Mach Intell.* 2013;35(8):1798-828.
- [50] Madhulatha TS. An overview on clustering methods. arXiv preprint arXiv:12051117. 2012.
- [51] Lloyd S. Least squares quantization in PCM. *IEEE Trans Inf Theory.* 1982;28(2):129-37.
- [52] Berrevoets J, Jordon J, Bica I, van der Schaar M. OrganITE: Optimal transplant donor organ offering using an individual treatment effect. *NIPS.* 2020;33:20037-50.
- [53] Wu J. Advances in K-means clustering: a data mining thinking. Springer Science & Business Media; 2012.

- [54] Hornik K, Stinchcombe M, White H. Multilayer feedforward networks are universal approximators. *Neural netw.* 1989;2(5):359-66.
- [55] Hastie T, Tibshirani R, Friedman JH, Friedman JH. *The elements of statistical learning: data mining, inference, and prediction.* vol. 2. Springer; 2009.
- [56] Kantorovich LV. Mathematical methods of organizing and planning production. *Manage Sci.* 1960;6(4):366-422.
- [57] Vaserstein LN. Markov processes over denumerable products of spaces, describing large systems of automata. *Problemy Peredachi Informatsii.* 1969;5(3):64-72.
- [58] Gretton A, Borgwardt K, Rasch M, Schölkopf B, Smola A. A kernel method for the two-sample-problem. *NIPS.* 2006;19.
- [59] Zhu Y, Savage JS, Ghosh D. A kernel-based metric for balance assessment. *J Causal Inference.* 2018;6(2):20160029.
- [60] Bishop CM, Nasrabadi NM. *Pattern recognition and machine learning.* vol. 4. Springer; 2006.
- [61] Curth A, van der Schaar M. In Search of Insights, Not Magic Bullets: Towards Demystification of the Model Selection Dilemma in Heterogeneous Treatment Effect Estimation. *arXiv preprint arXiv:230202923.* 2023.
- [62] The Cancer Genome Atlas Research Network, Weinstein JN, Collisson EA, Mills Shaw KR, Ozenberger BA, Ellrott K, et al. The cancer genome atlas pan-cancer analysis project. *Nat genet.* 2013;45(10):1113-20.
- [63] Johansson F, Shalit U, Sontag D. Learning representations for counterfactual inference. In: *ICML.* PMLR; 2016. p. 3020-9.
- [64] Paszke A, Gross S, Chintala S, Chanan G, Yang E, DeVito Z, et al. Automatic differentiation in PyTorch. In: *NIPS-W;* 2017. p. 1-4.
- [65] Seabold S, Perktold J. statsmodels: Econometric and statistical modeling with python. In: *9th Python in Science Conference;* 2010. p. 92-6.
- [66] Galagate D. Causal inference with a continuous treatment and outcome: Alternative estimators for parametric dose-response functions with applications; 2016.
- [67] R Core Team. *R: A Language and Environment for Statistical Computing.* Vienna, Austria; 2022.
- [68] VanderWeele TJ, Hernan MA. Causal inference under multiple versions of treatment. *J Causal Inference.* 2013;1(1):1-20.
- [69] Berrevoets J, Verboven S, Verbeke W. Treatment effect optimisation in dynamic environments. *J Causal Inference.* 2022;10(1):106-22.

A Hyperparameters

All models trained for the experiments in this manuscript have been trained on a set of different hyperparameters as described below.

Table A1: Hyperparameters DRNet

Parameter	Values
Dose strata	{10}
Number of representation layers	{2}
Number of inference layers	{2}
Nodes per hidden layer	{32}
Batch size	{32, 48}
Learning rate	{0.01, 0.05}

Table A2: Hyperparameters MLP

Parameter	Values
Number of hidden layers	{2}
Nodes per hidden layer	{32}
Batch size	{32, 48}
Learning rate	{0.01, 0.05}

Table A3: Hyperparameters CBRNet

Parameter	Values
Number of representation layers	{2}
Number of inference layers	{2}
Number of clusters	{5}
Nodes per hidden layer	{32}
Batch size	{32, 48}
Learning rate	{0.01, 0.05}
λ	{0.0, 0.5, 5.0, 50.0}

B Figures

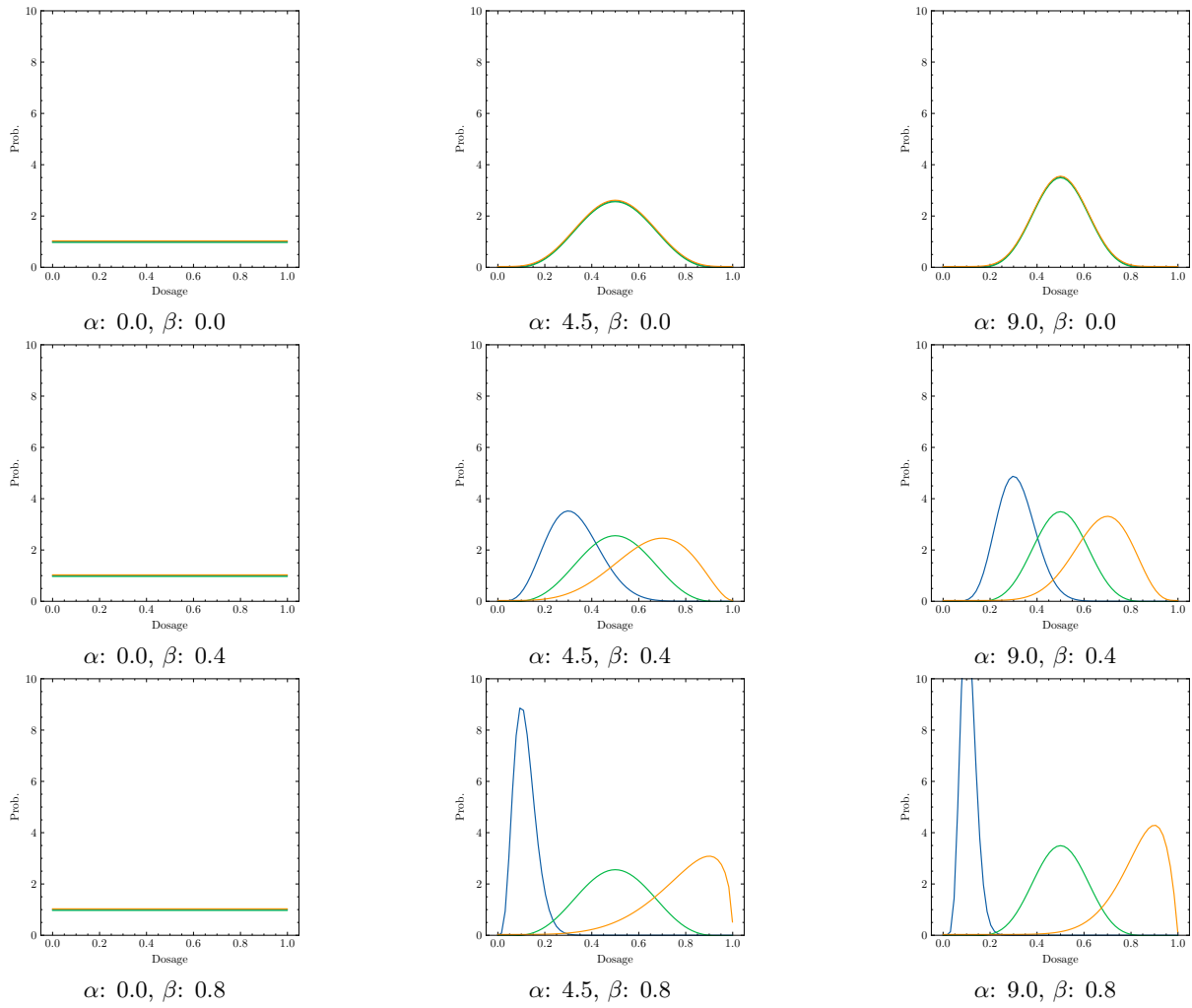


Figure A1: Implication of different levels of dose selection bias on observed doses per $k = 3$ clusters

C Tables

Table A4: MISE per method for fixed levels of α and varying levels of β

$\alpha = 0.0$					
Model	β				
	0.0	0.2	0.4	0.6	0.8
MLP	0.54 ± 0.06	0.54 ± 0.06	0.54 ± 0.06	0.54 ± 0.06	0.54 ± 0.06
HIE	0.71 ± 0.04	0.71 ± 0.04	0.71 ± 0.04	0.71 ± 0.04	0.71 ± 0.04
DRNet	0.64 ± 0.02	0.64 ± 0.02	0.64 ± 0.02	0.64 ± 0.02	0.64 ± 0.02
VCNet	0.19 ± 0.02	0.19 ± 0.02	0.19 ± 0.02	0.19 ± 0.02	0.19 ± 0.02
CBRNet	0.29 ± 0.04	0.29 ± 0.04	0.29 ± 0.04	0.29 ± 0.04	0.29 ± 0.04

$\alpha = 6.0$					
Model	β				
	0.0	0.2	0.4	0.6	0.8
MLP	2.46 ± 0.20	2.14 ± 0.21	1.65 ± 0.49	1.45 ± 0.57	1.64 ± 0.50
HIE	3.16 ± 0.05	2.92 ± 0.11	2.65 ± 0.31	2.59 ± 0.31	2.55 ± 0.23
DRNet	1.87 ± 0.15	1.62 ± 0.16	1.37 ± 0.11	1.18 ± 0.09	0.83 ± 0.10
VCNet	2.22 ± 0.07	1.80 ± 0.22	1.38 ± 0.28	0.87 ± 0.30	0.43 ± 0.14
CBRNet	2.07 ± 0.17	1.43 ± 0.33	0.96 ± 0.21	0.69 ± 0.23	0.81 ± 0.97

$\alpha = 9.0$					
Model	β				
	0.0	0.2	0.4	0.6	0.8
MLP	3.09 ± 0.26	2.42 ± 0.36	2.12 ± 0.39	1.84 ± 0.79	1.50 ± 0.61
HIE	3.76 ± 0.04	3.42 ± 0.18	2.97 ± 0.36	2.79 ± 0.34	2.56 ± 0.18
DRNet	2.03 ± 0.23	2.01 ± 0.20	1.62 ± 0.16	1.33 ± 0.10	0.88 ± 0.19
VCNet	2.58 ± 0.22	2.27 ± 0.15	1.68 ± 0.27	0.98 ± 0.31	0.50 ± 0.20
CBRNet	2.75 ± 0.24	1.98 ± 0.17	1.37 ± 0.18	1.00 ± 0.31	0.79 ± 0.65

Table A5: MISE per method for fixed levels of β and varying levels of α

$\beta = 0.0$				
Model	α			
	0.0	3.0	6.0	9.0
MLP	0.54 \pm 0.06	1.42 \pm 0.31	2.46 \pm 0.20	3.09 \pm 0.26
HIE	0.71 \pm 0.04	2.06 \pm 0.04	3.16 \pm 0.05	3.76 \pm 0.04
DRNet	0.64 \pm 0.02	1.32 \pm 0.10	1.87 \pm 0.15	2.03 \pm 0.23
VCNet	0.19 \pm 0.02	<i>1.24</i> \pm 0.07	2.22 \pm 0.07	<i>2.58</i> \pm 0.22
CBRNet	<i>0.29</i> \pm 0.04	0.97 \pm 0.20	<i>2.07</i> \pm 0.17	2.75 \pm 0.24

$\beta = 0.2$				
Model	α			
	0.0	3.0	6.0	9.0
MLP	0.54 \pm 0.06	1.25 \pm 0.30	2.14 \pm 0.21	2.42 \pm 0.36
HIE	0.71 \pm 0.04	2.05 \pm 0.03	2.92 \pm 0.11	3.42 \pm 0.18
DRNet	0.64 \pm 0.02	1.15 \pm 0.12	<i>1.62</i> \pm 0.16	<i>2.01</i> \pm 0.20
VCNet	0.19 \pm 0.02	<i>1.12</i> \pm 0.17	1.80 \pm 0.22	2.27 \pm 0.15
CBRNet	<i>0.29</i> \pm 0.04	0.77 \pm 0.15	1.43 \pm 0.33	1.98 \pm 0.17

$\beta = 0.6$				
Model	α			
	0.0	3.0	6.0	9.0
MLP	0.54 \pm 0.06	0.91 \pm 0.18	1.45 \pm 0.57	1.84 \pm 0.79
HIE	0.71 \pm 0.04	2.34 \pm 0.13	2.59 \pm 0.31	2.79 \pm 0.34
DRNet	0.64 \pm 0.02	0.95 \pm 0.14	1.18 \pm 0.09	1.33 \pm 0.10
VCNet	0.19 \pm 0.02	<i>0.64</i> \pm 0.23	<i>0.87</i> \pm 0.30	0.98 \pm 0.31
CBRNet	<i>0.29</i> \pm 0.04	0.53 \pm 0.13	0.69 \pm 0.23	<i>1.00</i> \pm 0.31

$\beta = 0.8$				
Model	α			
	0.0	3.0	6.0	9.0
MLP	0.54 \pm 0.06	0.97 \pm 0.26	1.64 \pm 0.50	1.50 \pm 0.61
HIE	0.71 \pm 0.04	2.43 \pm 0.11	2.55 \pm 0.23	2.56 \pm 0.18
DRNet	0.64 \pm 0.02	0.75 \pm 0.09	0.83 \pm 0.10	0.88 \pm 0.19
VCNet	0.19 \pm 0.02	0.37 \pm 0.16	0.43 \pm 0.14	0.50 \pm 0.20
CBRNet	<i>0.29</i> \pm 0.04	<i>0.39</i> \pm 0.14	<i>0.81</i> \pm 0.97	<i>0.79</i> \pm 0.65